Clays and Clay Minerals, Vol. 49, No. 4, 310–317, 2001.

A HRTEM STUDY OF CRONSTEDTITE: DETERMINATION OF POLYTYPES AND LAYER POLARITY IN TRIOCTAHEDRAL 1:1 PHYLLOSILICATES

TOSHIHIRO KOGURE,[1] JIŘÍ HYBLER[2] AND SLAVOMIL ĎUROVIČ[3]

[1]Department of Earth and Planetary Science, Graduate School of Science, the University of Tokyo, 7-3-1 Hongo, Bunkyoku, Tokyo 113-0033, Japan

[2]Institute of Physics, Science Academy of the Czech Republic, Na Slovance 2, CZ-18221, Praha 8, Czech Republic

[3]Institute of Inorganic Chemistry, Slovak Academy of Sciences, SK-84236 Bratislava, Slovak Republic

Abstract—It is shown that polytypes or stacking sequences of cronstedtite, an Fe-bearing trioctahedral 1:1 phyllosilicate, can be determined using near-atomic high-resolution transmission electron microscopy (HRTEM). By viewing along the [010], [310] and [3$\bar{1}$0] directions (orthohexagonal indexing), the four groups of the standard polytypes can be distinguished. Imaging along the [100], [110] and [1$\bar{1}$0] directions allows determination of the polytypes in each group. The polytypic sequences of groups A and C are intergrown at the monolayer level in cronstedtite from Lostwithiel, England, which is a new insight if compared with previous suggestions that layer stackings characteristic of different groups do not occur together. The HRTEM images also revealed the relationship between the layer polarity and the morphology of the cronstedtite crystals, where the tetrahedral sheet side points towards the top of the truncated pyramidal shape of the crystal.

Key Words—Cronstedtite, HRTEM, Layer Polarity, Morphology, Polytype, Stacking Disorder, Trioctahedral 1:1 Phyllosilicates

INTRODUCTION

Polytypism is closely related to the formation and identification of minerals. In the case of micas, it is caused by rotation between adjacent 2:1 layers by a multiple of 60°. The polytypism of chlorites or of 1:1 phyllosilicates is more complicated because another variable, namely different stacking geometries at hydrogen bonding at the interlayer regions, also occurs. Bailey (1969) derived theoretically 12 standard polytypes for trioctahedral 1:1 phyllosilicates. These polytypes are divided into four groups termed A, B, C and D, which are distinguished by the shift and rotation between adjacent layers; $\pm a_i/3$ shifts for group A, $\pm a_i/3$ shifts combined with 180° rotation for group B, $\pm b/3$ or no shift for group C, $\pm b/3$ or no shift combined with 180° rotation for group D, where a_i and b correspond to the lengths of the edges of hexagonal and orthohexagonal cells, respectively. Zvyagin (1964, 1967) and Zvyagin *et al.* (1979) also derived the four groups for 1:1 phyllosilicates, including 12 trioctahedral and 36 dioctahedral standard—in his terminology "homogeneous"—polytypes. An order-disorder (OD) interpretation of 1:1 phyllosilicates was given by Dornberger-Schiff and Ďurovič (1975a, b); the results were four sub-families (groups) and 12 trioctahedral maximum-degree-of-order (MDO) polytypes identical to those given by Bailey (1969) and Zvyagin (1964, 1967).

Disordered or heavily twinned specimens of these phyllosilicates are common, and conventional diffraction techniques are not effective for investigating the polytypic sequences in them. Generally, polytypes within each group mix easily to form disordered stacking sequences because the energy difference between them is evidently much smaller than that between different groups. Kogure and Banfield (1998) showed that the six groups of chlorites could be distinguished directly in the images by near-atomic high-resolution transmission electron microscopy (HRTEM) along the [010], [310] and [3$\bar{1}$0] directions, which had scarcely been applied in previous TEM work because very high resolution is required along these directions. Those authors discovered that the geometry of the hydrogen bonding and the slant direction of the octahedral sheets within the interlayer regions and within the 2:1 layers can be determined from HRTEM images with a point resolution of ~0.2 nm. They also reported that stacking sequences of various groups are intergrown in chlorite packets within hydrothermally altered biotite from granite (Kogure and Banfield, 2000). This technique can also be used to identify the polytypes in 1:1 phyllosilicates. However, common 1:1 phyllosilicates, *e.g.* kaolin or serpentine subgroups, are so prone to damage by electron beam radiation that images with such a high resolution are only recorded with great difficulty. The curved layering in some of these minerals is also an obstacle for such observations. In our experience, Fe-bearing phyllosilicates were, in general, more tolerant of beam radiation than Mg- or Al-bearing phyllosilicates. In the case of micas, for instance, this tolerance decreased in the sequence: annite > phlogopite > muscovite. Cronstedtite is a planar trioctahedral 1:1 phyllosilicate containing mainly ferrous and ferric iron in the octahedral sites and ferric iron and Si in the tetrahedral sites, with a generalized chemical formula of $(Fe^{2+}_{3-x}, Fe^{3+}_{x})^{VI}(Si_{2-x}, Fe^{3+}_{x})^{IV}O_5(OH)_4$, where x was

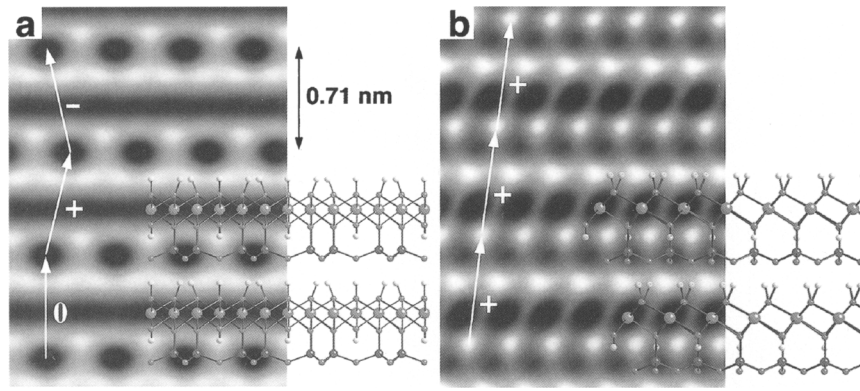

Figure 1. Relation between the structure of cronstedtite-3*T* and its simulated contrasts in HRTEM images observed down (a) [100] and (b) [010] (orthohexagonal indexing). The specimen thickness and defocus value for the simulation are 2.5 nm and −42 nm (Scherzer defocus), respectively. The arrows connect equivalent sites in adjacent layers and the signs ('0', '+', and '−') indicate the stagger directions from the underlayer.

reported to be in the range of 0.5–0.8 in previous works (Geiger *et al.*, 1983; Smrčok *et al.*, 1994; Hybler *et al.*, 2000). It was found in the present investigation that this mineral is resistant to beam damage during HRTEM examination. Cronstedtite is also suitable for the investigation of polytypism because it exhibits a variety of polytypes except those in group B (Frondel, 1962; Steadman and Nuttall, 1963, 1964). Actually no Group B polytype has yet been found among 1:1 phyllosilicates. This paper describes how to identify polytypes in trioctahedral 1:1 phyllosilicates by HRTEM and reports some polytypic aspects found in disordered cronstedtite from several localities. Furthermore, the relationship between the crystal structure and the morphology of cronstedtite, determined by HRTEM, is also presented.

MATERIALS AND METHODS

Materials

Cronstedtite samples from several localities were investigated for this study and two of them, from Kutná Hora, Bohemia, Czech Republic (Smrčok *et al.*, 1994) and from Lostwithiel, Cornwall, England (Hybler *et al.*, 2000) are described in the next section. Crystals for TEM observation were examined using X-ray precession photographs to identify polytypes or groups. Electron probe microanalyses (EPMA) indicated that the chemical compositions of the two samples were identical to those reported in previous works (Smrčok *et al.*, 1994; Hybler *et al.*, 2000) within standard deviation. X-ray precession photographs showed that the Kutná Hora sample contained two kinds of crystals, belonging to groups A and D, respectively; the latter was relatively rare. They were easily distinguished by their crystal morphologies; the group A crystals have a truncated triangular pyramidal shape whereas the group D crystals are usually almost columnar with a circular or rounded-hexagonal cross-section. Analysis of EPMA indicated no compositional difference between the two crystals types.

Methods

The specimens for TEM observation along the [*hk*0] directions (parallel to the (001) plane) were prepared by ion-milling, as described by Kogure and Murakami (1998). The TEM observations were performed at 200 kV using a JEOL JEM-2010 microscope with a LaB_6 filament, a high-resolution pole-piece (nominal point resolution of 0.20 nm), and a double-tilt specimen holder used to rotate the specimen by up to ±20°. All HRTEM images were recorded around thin specimen areas near Scherzer defocus, which enables the interpretation of images with dark contrast corresponding to large charge potentials. Some of the experimental images recorded on films were digitized using a CCD camera and processed by rotational filtering (Kilaas, 1998) implemented within Gatan Digital-Micrograph version 2.5 (see the next section). The image simulation was performed using MacTempas software (Total Resolution Co.). The crystal parameters reported by Steadman and Nuttall (1963) were used for the simulation.

RESULTS AND DISCUSSION

Identification of the polytypes by HRTEM

Figure 1 shows the schematic structure and the corresponding contrast in simulated HRTEM images of cronstedtite-3*T* observed along two principal directions. In the present study, orthohexagonal indexing was adopted instead of hexagonal in order to maintain a constant indexing system with polytypes whose symmetry is neither trigonal nor hexagonal. The three axial directions [100], [110] and [1$\bar{1}$0] are equivalent in the trigonal or hexagonal systems, and are expressed as [100]/[110]/[1$\bar{1}$0]. Likewise, the three inter-axial di-

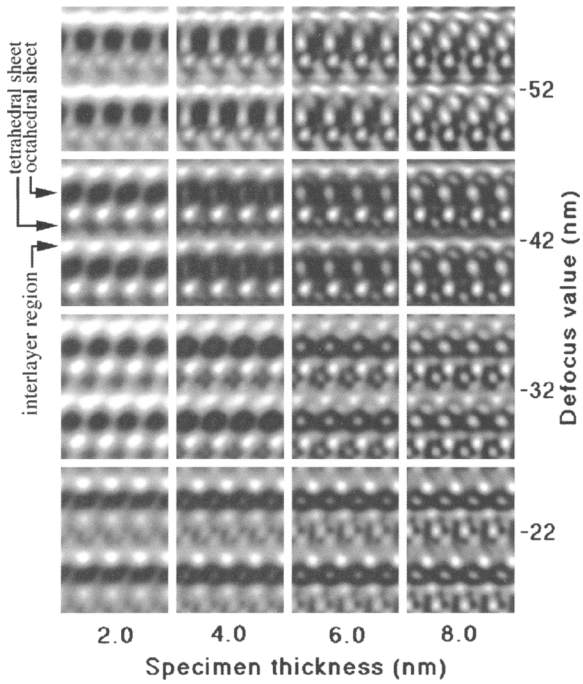

Figure 2. Matrix of the simulated images of cronstedtite-1*T* recorded down [010], as functions of the specimen thickness and defocus value.

rections [010], [310] and [3$\bar{1}$0] are represented as [010]/[310]/[3$\bar{1}$0]. Observations along the three directions in the two sets show the same contrast at each 1:1 unit layer because each layer individually possesses trigonal symmetry, $P31m$. In the images observed along [100]/[110]/[1$\bar{1}$0], the octahedral sheet shows a continuous dark contrast and the tetrahedral sheet consists of dark spots separated by $b/2$ (any layer is *C*-centered in the orthohexagonal system); these dark spots correspond to a pair of tetrahedra (Figure 1a) (Banfield *et al.*, 1994). On the other hand, in the image observed along [010]/[310]/[3$\bar{1}$0] (Figure 1b), the octahedral sheet consists of dark oval spots, each of which corresponds to one octahedron, and each tetrahedron in the tetrahedral sheet is resolved as a dark spot separated by $a/2$. The displacement in the a–b plane between adjacent layers in polytypes of groups A and B is $\pm a_i/3$ (with i = 1, 2, 3, hexagonal axes), which generates the stagger of $a/6$ between adjacent layers if observed along [010]/[310]/[3$\bar{1}$0] (Figure 1b). On the other hand, in the case of groups C and D the displacement is zero or $\pm b/3$, which generates no stagger in the images observed along [010]/[310]/[3$\bar{1}$0] (see Figure 2 or the inset in Figure 3b). Next, the slant directions of octahedra, or the orientational parity of 1:1 layers (Dornberger-Schiff and Ďurovič, 1975a, 1975b), can be identified by the inclination of the oval or by the stagger direction between the dark oval of the octahedron and the spot of the tetrahedron within a 1:1 layer (Figure 1b). As the slant directions of the octahedra or the orientational parities are either the same (groups A and C) or regularly alternating (B and D) between adjacent layers, groups A and B (or C and D) can be distinguished. Consequently, the four groups can be distinguished by the HRTEM images recorded along [010]/[310]/[3$\bar{1}$0], as is the case with chlorite (Kogure and Banfield, 1998).

The polytypes within each group can be distinguished in the HRTEM images along [100]/[110]/[1$\bar{1}$0] as follows. The displacement of $\pm a_i/3$ between

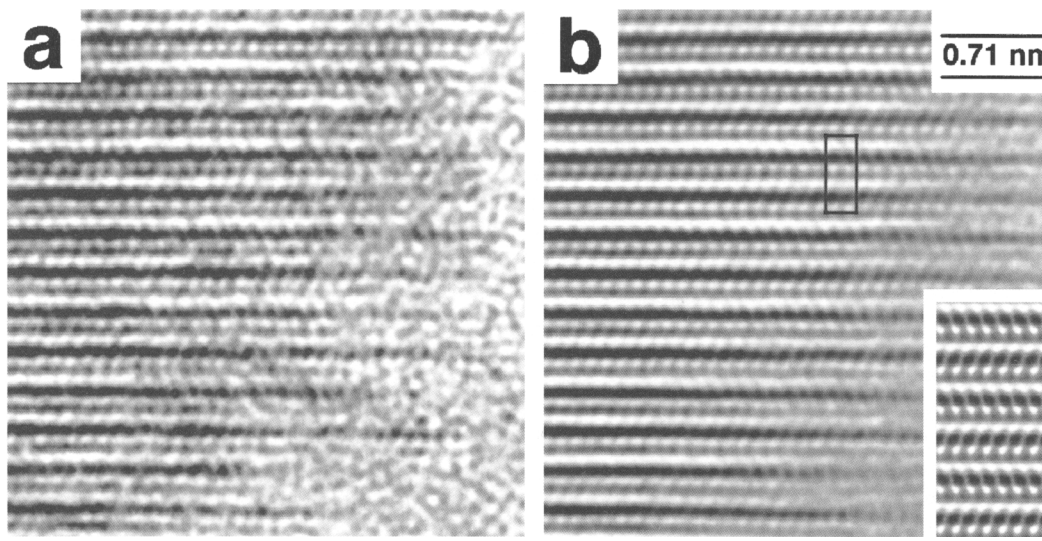

Figure 3. (a) Observed and (b) filtered images of cronstedtite from Kutná Hora (group D), recorded along [010]/[310]/[3$\bar{1}$0]. The square in (b) indicates an orthohexagonal unit-cell of $2H_1$ or $2H_2$. The inset at the bottom-right in (b) is the simulated contrast for the group D structure at Scherzer defocus and specimen thickness of 2.5 nm.

Table 1. Possible stagger sequences of the 12 standard polytypes observed along [100], [$\bar{1}$00] and the four related directions (see Figure 1a for the definition of the characters 0, +, −). Identical sequences are given only once.

Group	Polytype	Stagger sequences
A	1*M*	000000, ++++++, −−−−−−
	$2M_1$	0+0+0+, 0−0−0−, +−+−+−
	3*T*	0+−0+−, 0−+0−+
B	2*O*	000000, +−+−+−
	$2M_2$[1]	0+0+0+, 0−0−0−, ++++++, −−−−−−
	6*H*	0++0−−
C	1*T*	000000
	2*T*	+−+−+−
	3*R*	++++++, −−−−−−
D	$2H_1$	000000
	$2H_2$	+−+−+−
	6*R*	++++++, −−−−−−

[1] The directions are [010] and related ones in the case of the $2M_2$ cell.

adjacent layers along the three directions in groups A and B forms no stagger or a stagger of $\pm b/6$ in the image contrast, depending upon the direction of displacement. The displacement of $\pm b/3$ in groups C and D also results in a stagger of $\pm b/6$ in the images along [100]/[110]/[1$\bar{1}$0]. If the staggers of zero, $+b/6$ and $-b/6$ are expressed as "0", "+", and "−" respectively (Baronnet and Kang, 1989, see also Figure 1a), possible sequences of these staggers for the 12 standard polytypes observed along six directions ([100]/[110]/[1$\bar{1}$0] and their reversed directions) are expressed as shown in Table 1. It is found that the same sequence does not appear between the polytypes in the same group. Consequently, the 12 standard polytypes are distinguished by the two images recorded along one axis of [010]/[310]/[3$\bar{1}$0] and of [100]/[110]/[1$\bar{1}$0].

Figure 2 shows simulated images of cronstedtite-1*T* along [010] as functions of the specimen thickness and defocus value. Dark oval contrast corresponding to an octahedron is distinguishable only at a specimen thickness <6 nm and proper defocus. This result indicates that a very thin specimen area, generally near the edge of holes formed by ion-milling, must be selected for the direct identification of polytypic sequences. Normally, ion-milling forms damaged amorphous material at the surface of the specimen and contrast from such amorphous layers smears the contrast from the crystal. This is especially critical in thin areas where informative contrast can be obtained. To remove such contrast from the amorphous surface, a filtering process is often necessary (Banfield and Murakami, 1998; Kogure and Banfield, 1998), especially for the images recorded along [010]/[310]/[3$\bar{1}$0] because of their fine structure.

Figures 3 and 4 represent examples of observed images. Figure 3 shows an original (Figure 3a) and a

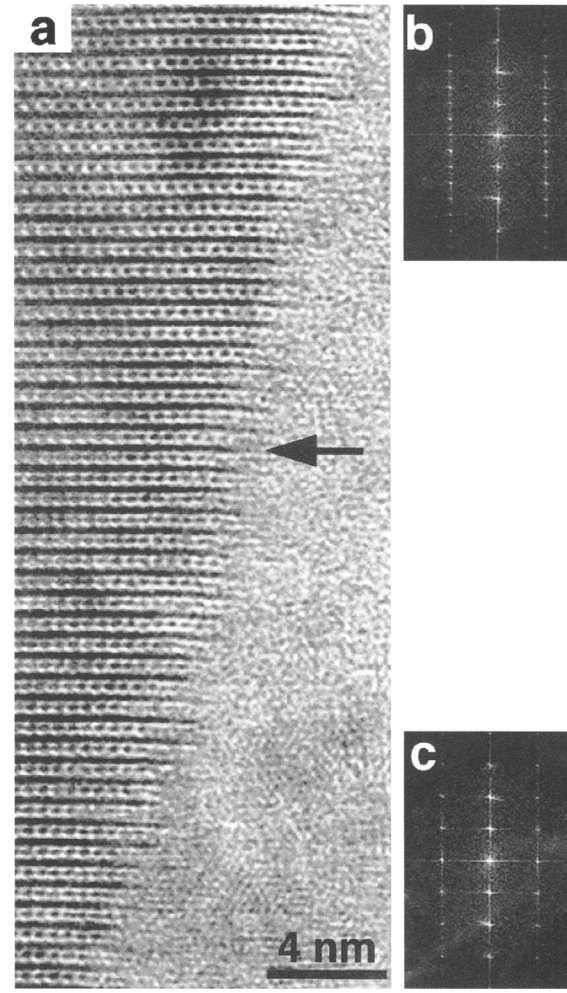

Figure 4. (a) HRTEM image of the same specimen as in Figure 3, recorded along [100]/[110]/[1$\bar{1}$0]. (b, c) Fourier transforms of the areas (b) above and (c) below the arrow in (a), showing (b) two-layer and (c) one-layer periodicities. Note that the layers are curved near the edge of the specimen (the right side in (a), and slight arcing of 00*l* spots in (b) and (c)). This is probably due to the mismatch of the lateral dimension between the octahedral and tetrahedral sheets in a 1:1 layer, and weakening of interlayer hydrogen bonding.

filtered (Figure 3b) HRTEM image of cronstedtite from Kutná Hora (group D), recorded along [010]/[310]/[3$\bar{1}$0]. In the original image, the contrast from the crystal is too smeared to determine the polytype. On the other hand, alternating slant directions within octahedral sheets and the absence of stagger between adjacent layers are clearly identified in the thin area (the right side) in the filtered image, as expected from the simulated image (inset at the bottom-right in Figure 3b). Figure 4a shows an image of the same specimen as in Figure 3, recorded along [100]/[110]/[1$\bar{1}$0]. A stagger between adjacent layers does not exist except at one layer in the area below the arrow, indicating the $2H_1$ polytype according to Table 1, but the

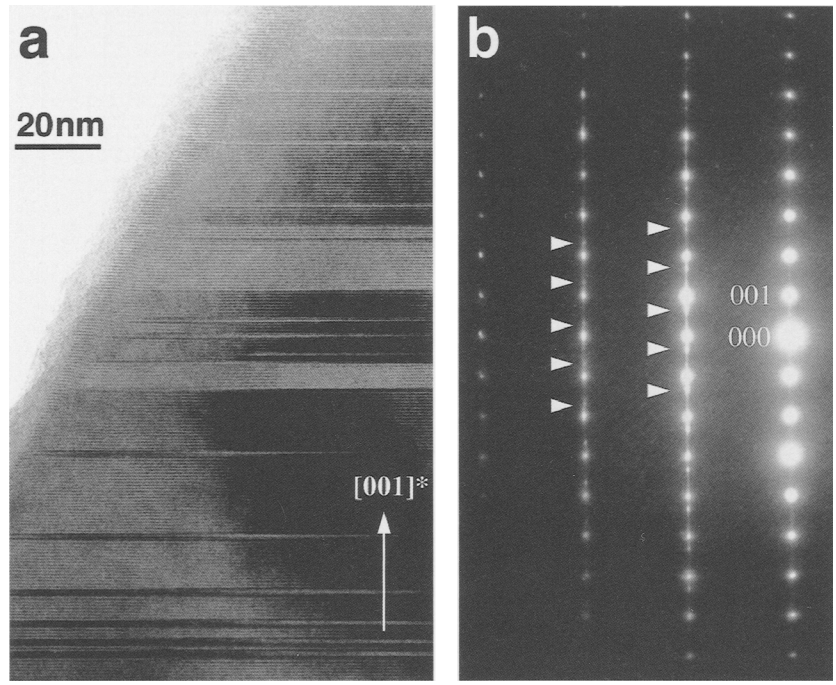

Figure 5. (a) Low-magnification bright-field image of cronstedtite from Lostwithiel, observed slightly away from [010]/[310]/[3$\bar{1}$0]. (b) Selected diffraction pattern from the area in (a). The diffraction spots of group A (indicated by the arrowheads) appear alongside those of group C.

stagger of '$-+-+-+$' is observed in the area above the arrow, indicating $2H_2$. As the diffraction spots of $2H_1$ are superimposed on those of $2H_2$, identification of the former polytype within the latter is virtually impossible by using conventional diffraction techniques. It is also noticed that the layers in Figure 4a are curved near the edge of the crystal (the right side), with the octahedral sheets outward. This is the same direction of curvature as is observed in chrysotile, which is caused by the misfit between octahedral and tetrahedral sheets. Hydrogen bonding between layers that suppresses bending of the layer is probably destroyed by electron beam radiation during observation or by ion bombardment during ion milling. The weak crossed lattice fringes are observed within the amorphous area near the edge of Figure 4a. Their spacing of 0.25 nm and crossing by 70° can be attributed to wüstite which was probably formed by electron beam radiation, since it has been reported that such metal oxides with the rock-salt structure were formed at the edge of TEM specimens by electron beam radiation (*e.g.* Banfield *et al.*, 1991; Kogure *et al.*, 1999).

Intergrowth of layer sequences belonging to different groups

Although it was recognized in previous work (*e.g.* Smrčok *et al.*, 1994) that polytypic disorder in cronstedtite is common, the simultaneous occurrence of different groups within the same crystal has not been reported. Steadman (1964) stated that such stacking does not occur. However, our HRTEM investigation of the cronstedtite specimen from Lostwithiel revealed that it does (XRO). Most specimens from Lostwithiel were identified on the basis of X-ray diffraction as more or less ordered group C crystals. One of them, which was very well ordered, was used for the refinement of the structure of the 1*T* polytype (Hybler *et al.*, 2000). On the other hand, heavily disordered crystals revealed in the X-ray work were used for TEM observation. Figure 5a shows a bright-field image at low magnification, recorded close to but slightly away from the [010]/[310]/[3$\bar{1}$0] orientation. It was reported that inhomogeneous stacking sequences can be distinguished by the distinctive image contrast observed in such diffraction conditions (Iijima and Buseck, 1978; Kogure and Nespolo, 1999a, b; Kogure and Banfield, 2000). The contrast in Figure 5a suggests that the crystal contains layers belonging to different stacking groups. Figure 5b shows the selected area electron diffraction pattern corresponding to Figure 5a but the zone axis was oriented exactly parallel to [010]/[310]/[3$\bar{1}$0]. In addition to the diffraction spots indicative of group C, weak spots identified as group A are observed as indicated by the arrowheads. Diffuse streaks along c* (accompanying reflections 20*l* and 40*l*, but not 60*l*) also suggest that the domains of groups A and C are intimately intergrown.

Figure 6 shows a filtered HRTEM image at a neighboring area in the same specimen. It can be seen that the

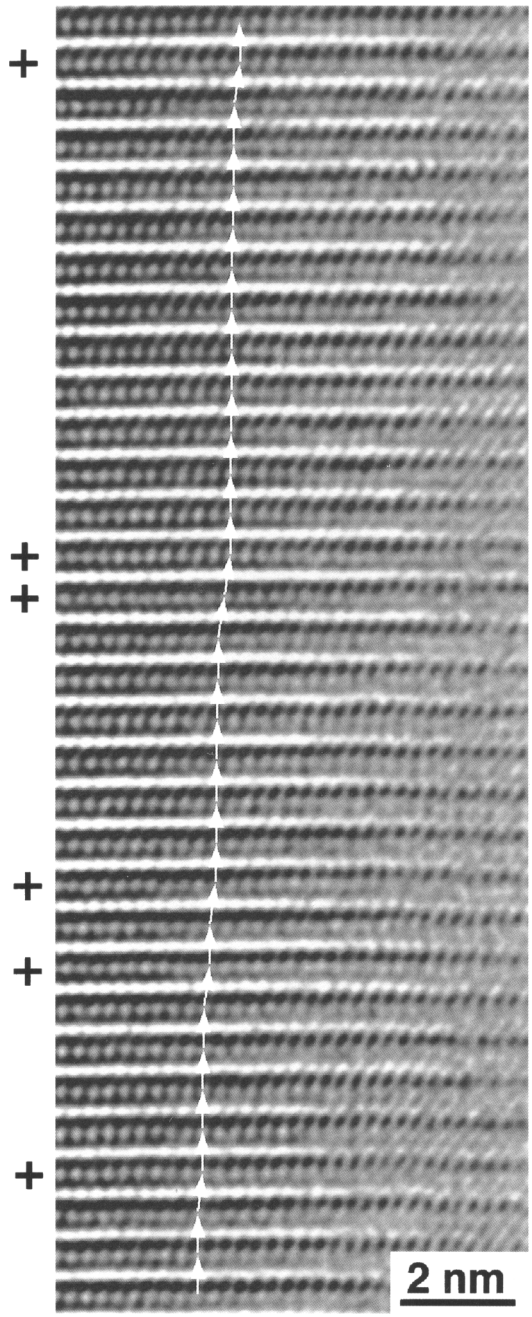

Figure 6. HRTEM image of the specimen in Figure 5, observed along [010]/[310]/[3$\bar{1}$0]. Layers marked with '+' are staggered by *a*/6 from the underlayer, showing the stacking sequence in group A, whereas the rest showing no stagger, is assigned to group C.

directions of the octahedral slant are the same for all layers, indicating that the stacking sequence of group B or D is not present, but the staggers between adjacent layers are disordered. The layers marked with '+' are staggered by *a*/6 from the underlayer whereas the other layers are not staggered. As described above, the sequences of layers with no stagger are identified as group C and with a stagger of *a*/6 as group A. Hence, it is concluded that the two groups are finely intergrown at the monolayer level in this specimen. The diffuse streaks in Figure 5b might be diagnostic of such intergrowth below the coherent size of diffracting domains, *i.e.* up to the monolayer level. Complete determination of the displacement between layers is possible by two HRTEM images from the same area along different directions (Kogure and Nespolo, 1999a, b). In this case, a marker (planar defects, microcleavage, *etc.*) is necessary to determine the correspondence of the same layer in the two images. It was found during our observations that one chlorite unit structure (a 2:1 layer plus an interlayer hydroxide sheet) was embedded in a disordered region of the specimen. Figure 7 shows HRTEM images along two directions separated by 30° (these directions are expressed tentatively as [100] and [310]), including the chlorite unit structure as a marker. Although the specimen is too thick to identify the direction of octahedral slant in the image along [310], the stagger between layers can be determined by the bright spots, which correspond to the channels between the octahedral and tetrahedral sheets, within a unit layer (Figure 1b). The layer displacements are derived from the two stagger directions

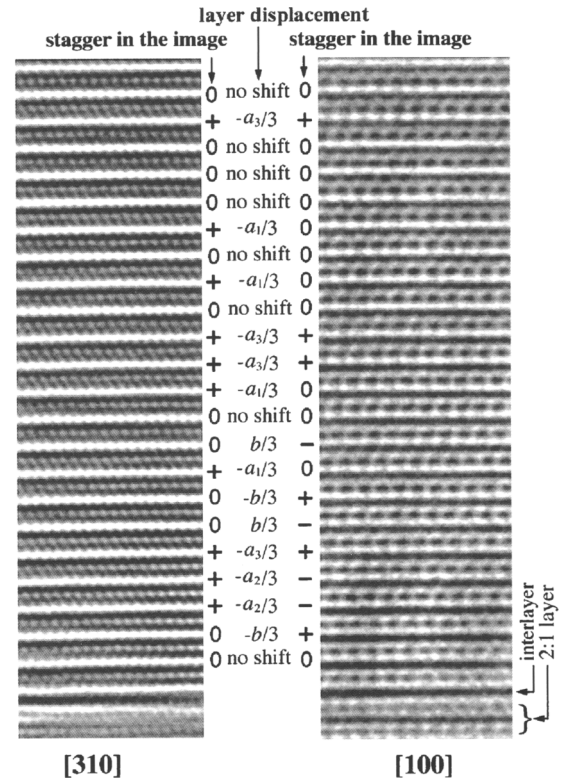

Figure 7. Two HRTEM images of the same area but recorded along two directions separated by 30°. One chlorite unit layer is identified at the bottom of the figures, which is used to identify the same layer in the two images (see text).

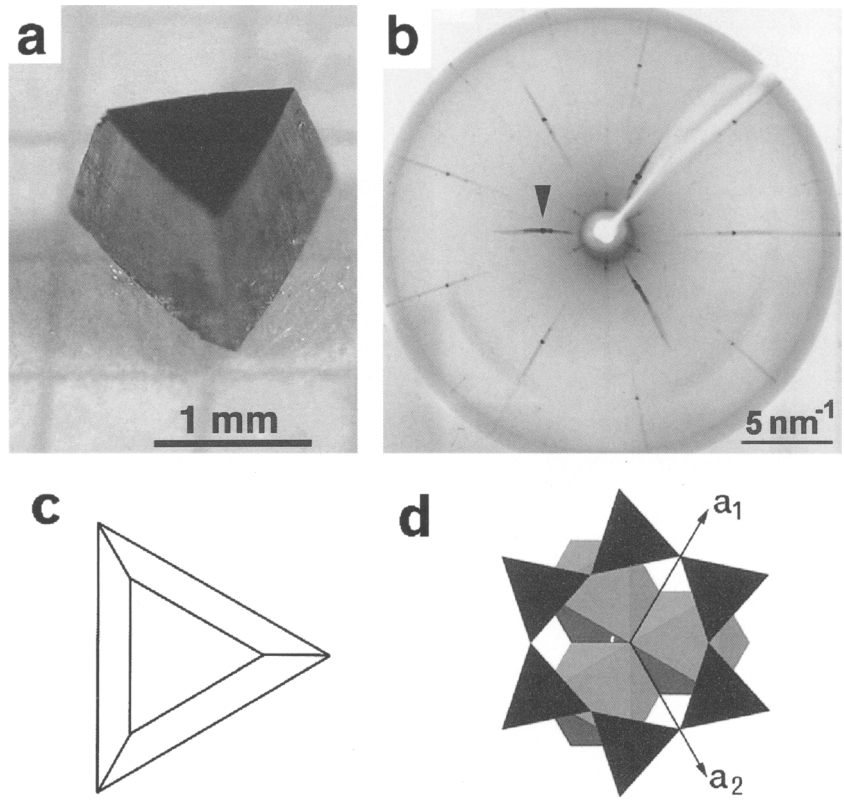

Figure 8. (a) Optical micrograph of the cronstedtite crystal from Kutná Hora (group A), showing a truncated triangular pyramidal shape. (b,c) X-ray precession photograph (b) of the $hk1$ or $hk\bar{1}$ reciprocal plane (the unit-cell of $3T$ is adopted) from the crystal in (a) with the crystal orientation as shown in (c). The precession photograph was taken with unfiltered Mo-K radiation. (d) Corresponding crystal structure to the morphology (c), determined by HRTEM images and the precession photograph in (b). The atomic parameters for cronstedtite-$3T$ by Smrčok *et al.* (1994) were used for the drawing.

for each layer (Figure 7). In conclusion, all kinds of displacements in groups A and C exist in this small area. Bailey (1988) discussed the relative stacking stabilities of the four groups in 1:1 phyllosilicates and suggested that the relative stability is in the order D>C>A>B. The present result suggests that the energy difference between groups A and C may not be so large or this specimen was formed under considerable disequilibrium.

The relationship between the crystal structure and morphology

Our HRTEM investigations turned out to be useful for determining the relationship between crystal structure and morphology. The 1:1 phyllosilicate structure is not centrosymmetric, and the direction of the polarity cannot be determined by routine diffraction techniques. Figure 8a shows a photograph of a crystal of cronstedtite-$3T$ from Kutná Hora (group A), exhibiting a truncated triangular pyramidal shape. This crystal morphology was also reported in lizardite ($1T$) in previous works (Mellini, 1982; Mellini and Zanazzi, 1987). An X-ray precession photograph of the $hk1$ or $hk\bar{1}$ reciprocal plane (the unit-cell of the $3T$ polytype ($P3_1$), is adopted) from the crystal in Figure 8a is shown in Figure 8b. Figure 8c illustrates the crystal orientation; the basal plane (0001) was perpendicular to the incident X-ray beam and one corner of the triangular basis plane pointed sideways, when the precession photograph was recorded. The calculation of diffraction intensities suggests that the strongest reflection as indicated by the arrowhead in Figure 8b is $11\bar{1}$ (or its equivalents) if the reciprocal plane is $hk1$, or $\bar{1}\bar{1}\bar{1}$ if it is $hk\bar{1}$. However, routine diffraction techniques cannot determine these alternatives because of Friedel's law.

A plate was taken from the crystal in Figure 8a by cleaving, and a cross-section specimen for TEM observation was prepared, distinguishing the top and bottom of the plate. The HRTEM images similar to those in previous figures indicated that the top of the pyramid corresponds to the tetrahedral side or the $-\mathbf{z}$ direction, and the bottom to the octahedral side or the $+\mathbf{z}$ in the cronstedtite structure. This result indicates that the reciprocal plane in Figure 8b is $hk\bar{1}$. In conclusion, the correspondence between the crystal morphology and structure is determined as shown in Figure 8c and 8d. The structure in Figure 8d was drawn using the atomic parameters for cronstedtite-$3T$, refined by Smrčok *et al.* (1994). The tetrahedral sheet in cronstedtite $-3T$ has a positive ditrigonalization angle (Franzini type A; Fran-

zini, 1969). The triangle of the (001) surface is antiparallel to the ditrigons formed by the basal oxygen atoms of the ditrigonalized tetrahedral sheets as well as to the triangular faces of octahedra adjacent to them (Figure 8d). Because the volume investigated by TEM was very limited (a few tens of micrometers along c*), the existence of large twinned domains might lead to false conclusions. More investigations on this topic are expected in future, probably using other techniques in addition to HRTEM, *e.g.* scanning probe microscopy.

ACKNOWLEDGMENTS

We are grateful to Dr M. Nespolo, National Institute for Research of Inorganic Materials, Japan for valuable discussions. We thank the Faculty of Sciences, Charles University, Prague, Czech Republic, for providing the Lostwithiel crystals (collection No. 3539). Crystals from Kutná Hora were provided by Dr K. Melka of the Geological Institute of the Academy of Sciences, Prague, Czech Republic. We are also grateful to Dr P. Heaney and Dr A. Baronnet for reviewing and improving the manuscript. The study was supported by grants 203/99/0067 and 202/00/0645 of the Grant Agency of the Czech Republic. Electron microscopy was carried out in the Electron Microbeam Analysis Facility of the Department of Earth and Planetary Science, University of Tokyo.

REFERENCES

Bailey, S.W. (1969) Polytypism of trioctahedral 1:1 layer silicates. *Clays and Clay Minerals,* **17,** 355–371.

Bailey, S.W. (1988) Polytypism of 1:1 layer silicates. Pp. 9–27 in: *Hydrous Phyllosilicates (Exclusive of Micas)* (S.W. Bailey, editor). Reviews in Mineralogy, **19.** Mineralogical Society of America, Washington, D.C.

Banfield, J.F. and Murakami, T. (1998) Atomic-resolution transmission electron microscope evidence for the mechanism by which chlorite weathers to 1:1 semi-regular chlorite-vermiculite. *American Mineralogist,* **83,** 348–357.

Banfield, J.F., Veblen, D.R. and Smith, D. J. (1991) The identification of naturally occurring TiO_2(B) by structure determination using high-resolution electron microscopy, image simulation, and distance-least-squares refinement. *American Mineralogist,* **76,** 343–353.

Banfield, J.F., Bailey, S.W. and Barker, W.W. (1994) Polysomatism, polytypism, defect microstructure, and relation mechanism in regularly and randomly interstratified serpentine and chlorite. *Contribution to Mineralogy and Petrology,* **117,** 137–150.

Baronnet, A. and Kang, Z.C. (1989) About the origin of mica polytypes. *Phase Transitions,* **16/17,** 477–493.

Dornberger-Schiff, K. and Ďurovič, S. (1975a) OD interpretation of kaolinite-type structures—I: Symmetry of kaolinite packets and their stacking possibilities. *Clays and Clay Minerals,* **23,** 219–229.

Dornberger-Schiff, K. and Ďurovič, S. (1975b) OD interpretation of kaolinite-type structures—II: The regular polytypes (MDO polytypes) and their derivation. *Clays and Clay Minerals,* **23,** 231–246.

Franzini, M. (1969) The A and B mica layers and the crystal structure of sheet silicates. *Contributions to Mineralogy and Petrology,* **21,** 203–224.

Frondel, C. (1962) Polytypism in cronstedtite. *American Mineralogist,* **47,** 781–783.

Geiger, C.A., Henry, D.L., Bailey, S.W. and Maj, J.J. (1983) Crystal structure of cronstedtite-2H_2. *Clays and Clay Minerals,* **31,** 97–108.

Hybler, J., Petříček, V., Ďurovič, S. and Smrčok, Ľ. (2000) Refinement of the crystal structure of the cronstedtite-1*T*. *Clays and Clay Minerals,* **48,** 331–338.

Iijima, S. and Buseck, P.R. (1978) Experimental study of disordered mica structures by high-resolution electron microscopy. *Acta Crystallographica,* **A34,** 709–719.

Kilaas, R. (1998) Optical and near-optical filters in high-resolution electron microscopy. *Journal of Microscopy,* **190,** 45–51.

Kogure, T. and Banfield, J.F. (1998) Direct identification of the six polytypes of chlorite characterized by semi-random stacking. *American Mineralogist,* **83,** 925–930.

Kogure, T. and Banfield, J.F. (2000) New insights into biotite chloritization mechanism via polytype analysis. *American Mineralogist,* **85,** 1202–1208.

Kogure, T. and Murakami, T. (1998) Structure and formation mechanism of low-angle grain boundaries in chlorite. *American Mineralogist,* **83,** 358–364.

Kogure, T. and Nespolo, M. (1999a) First finding of a stacking sequence with (±60°, 180°) rotation in biotite. *Clays and Clay Minerals,* **47,** 784–792.

Kogure, T. and Nespolo, M. (1999b) A TEM study of long-period mica polytypes: determination of the stacking sequence of oxybiotite by means of atomic-resolution images and Periodic Intensity Distribution (PID). *Acta Crystallographica,* **B55,** 507–516.

Kogure, T., Saiki, K., Konno, M. and Kamino, T. (1999) HRTEM and EELS studies of reacted materials from CaF_2 by electron beam irradiation. Pp. 183–188 in: *Atomistic Mechanisms in Beam Synthesis and Irradiation of Materials* (J.C. Barbour, S. Roorda, D. Ila and M. Tsujioka, editors). MRS Symposium Proceedings, **504.** Material Research Society, Pennsylvania.

Mellini, M. (1982) The crystal structure of lizardite 1*T*: hydrogen bonds and polytypism. *American Mineralogist,* **67,** 587–598.

Mellini, M. and Zanazzi, P.F. (1987) Crystal structures of lizardite-1*T* and lizardite-2*H*1 from Coli, Italy. *American Mineralogist,* **72,** 943–948.

Smrčok, Ľ., Ďurovič, S., Petříček, V. and Weiss, Z. (1994) Refinement of the crystal structure of cronstedtite-3*T*. *Clays and Clay Minerals,* **42,** 544–551.

Steadman, R. (1964) The structures of trioctahedral kaolin-type silicates. *Acta Crystallographica,* **17,** 924–927.

Steadman, R. and Nuttall, P.M. (1963) Polymorphism in cronstedtite. *Acta Crystallographica,* **16,** 1–8.

Steadmann, R. and Nuttall, P.M. (1964) Further polymorphism in cronstedtite. *Acta Crystallographica,* **17,** 404–406.

Zvyagin, B.B. (1964) *Electron Diffraction Analysis of Clay Mineral Structures.* Nauka Press, Moscow, 200 pp. (in Russian).

Zvyagin, B.B. (1967) *Electron Diffraction Analysis of Clay Mineral Structures.* Plenum Press, New York, 364 pp.

Zvyagin, B.B., Vrublevskaya, Z.V., Zhukhlistov, A.P., Sidorenko, O.V., Soboleva, S.V. and Fedotov, A.F. (1979) *High-voltage Electron Diffraction in the Study of Layered Minerals.* Nauka Press, Moscow, 224 pp. (in Russian).

E-mail of corresponding author: kogure@eps.s.u-tokyo.ac.jp

(*Received 22 June 2000; revised 22 February 2001; Ms. 463; A.E. Peter J. Heaney*)